Copper(IV) Complexes Hot Paper

International Edition: DOI: 10.1002/anie.201507330
German Edition: DOI: 10.1002/ange.201507330

Experimental and Theoretical Investigations of the Existence of Cu^{II}, Cu^{III}, and Cu^{IV} in Copper Corrolato Complexes

Woormileela Sinha, Michael G. Sommer, Naina Deibel, Fabian Ehret, Matthias Bauer, Biprajit Sarkar, and Sanjib Kar**

Abstract: *The most common oxidation states of copper in stable complexes are +I and +II. Cu^{III} complexes are often considered as intermediates in biological and homogeneous catalysis. More recently, Cu^{IV} species have been postulated as possible intermediates in oxidation catalysis. Despite the importance of these higher oxidation states of copper, spectroscopic data for these oxidation states remain scarce, with such information on Cu^{IV} complexes being non-existent. We herein present the synthesis and characterization of three copper corrolato complexes. A combination of electrochemistry, UV/Vis/NIR/EPR spectroelectrochemistry, XANES measurements, and DFT calculations points to existence of three distinct redox states in these molecules for which the oxidation states +II, +III, and +IV can be invoked for the copper centers. The present results thus represent the first spectroscopic and theoretical investigation of a Cu^{IV} species, and describe a redox series where Cu^{II}, Cu^{III}, and Cu^{IV} are discussed within the same molecular platform.*

The concept of formal oxidation states, even though sometimes criticized, forms an excellent basis for electron book keeping and often for the explanation of trends in chemical reactivity.[1] With regard to the latter, the pursuit of discovering the highest possible oxidation states for a particular element is a topic of high interest.[2] One reason for this quest is the involvement of metal centers in high oxidation states in various catalytic processes,[1b,2] with the water oxidation reaction being a prominent current example.[3] The most frequently encountered oxidation states of copper are 0 (usually in the metallic form) and +I and +II in metal complexes and salts.[4] Furthermore, Cu^{III} species have often been proposed as catalytic intermediates, and there are also few examples of well characterized Cu^{III} compounds.[5] Higher oxidation states of copper, such as Cu^{III}, are of great importance in copper-based high-temperature superconductors.[6] High-valent copper species, in this case organometallic Cu^{III} species, have been explored in carbon–carbon coupling reactions.[7] Theoretical calculations have suggested the involvement of Cu^{III} species in catalytic dioxygenation reactions with various monooxygenase enzymes.[8]

$Cs_2[CuF_6]$ is the oldest example of copper in the +IV oxidation state.[9] However, there are several limitations related to dealing with this compound, including its synthesis under harsh reaction conditions using an autoclave (at very high temperature and pressure) and its tendency to react vigorously with water and thereby decompose.[9] If we ignore these rare examples of Cu^{IV} species in the solid, such as the fluoride cuprates, then, to the best of our knowledge, no examples of copper in the +IV oxidation state have been described. Recent reports on the use of copper complexes for the water oxidation reaction have invoked the involvement of a formal Cu^{IV} oxidation state in the proposed catalytic cycle.[10] However, no experimental evidence has yet been collected on the existence of such species. It is indeed true that the observation of the oxidation state +IV is very rare in copper chemistry. The rich and extensive application of higher oxidation states of copper certainly suggests that the high-valent copper species (Cu^{IV}) might even be relevant in nature. The discovery of a new higher oxidation state of an abundant (in the earth's crust) non-precious metal, such as copper, can open up entirely new avenues for chemical reactivity.

Corroles in their deprotonated forms are known to stabilize transition metals in high oxidation sates.[11] In many cases, unusually high oxidation states that are unlikely to be stabilized by other ligand environments are found to be stable inside the corrolato cavity. The trianionic nature of the corrolato ligand is certainly helpful for this purpose. Some of the higher oxidation states of metals that have been stabilized in corrolato environments include Cu^{III}, Ag^{III}, Fe^{IV}, Co^{IV}, Co^{V}, Cr^{V}, and Cr^{VI}.[12]

We have recently presented unambiguous experimental and theoretical evidence for the existence of Ag^{II} and Ag^{III} within the same corrolato framework.[13] In the following, we present the synthesis of three new copper complexes [5,10,15-tris(4-cyanophenyl)corrolatocopper(III) (**1**), 10-(2,4,5-trimethoxyphenyl)-5,15-bis(4-cyanophenyl)corrolatocopper(III)

[*] W. Sinha,[+] Dr. S. Kar
School of Chemical Sciences
National Institute of Science Education and Research (NISER)
Bhubaneswar, 751005 (India)
E-mail: sanjib@niser.ac.in
M. G. Sommer,[+] N. Deibel, Prof. Dr. B. Sarkar
Institut für Chemie und Biochemie
Anorganische Chemie
Freie Universität Berlin
Fabeckstrasse 34–36, 14195 Berlin (Germany)
E-mail: biprajit.sarkar@fu-berlin.de
N. Deibel, F. Ehret
Institut für Anorganische Chemie
Universität Stuttgart
Pfaffenwaldring 55, 70569 Stuttgart (Germany)
Prof. Dr. M. Bauer
Universität Paderborn
Naturwissenschaftliche Fakultät, Department Chemie
Warburger Strasse 100, 33098 Paderborn (Germany)
[+] These authors contributed equally to this work.

Supporting information for this article is available on the WWW under http://dx.doi.org/10.1002/anie.201507330.

(**2**), and 10-(4,7-dimethoxynaphthalen-1-yl)-5,15-bis(4-cyanophenyl)corrolatocopper(III) (**3**)] with corrolato ligands that are symmetrically as well as non-symmetrically substituted.

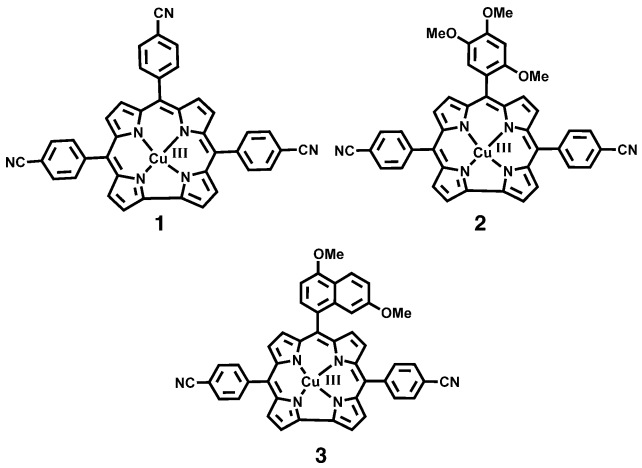

An approach combining synthetic, electrochemical, UV/Vis/NIR/EPR spectroelectrochemical, crystallographic, and DFT studies has been adapted to establish the origin of Cu^{II}, Cu^{III}, and Cu^{IV} within the three-step redox series of these complexes.

The Cu^{III} corrolato derivatives were synthesized by slight modifications of a reported procedure.[14] The respective corroles were dissolved in pyridine and stirred with excess copper(II) acetate hydrate to yield the corresponding Cu^{III} corrolato derivatives **1**, **2**, and **3**. Their purity and identity were demonstrated by satisfactory elemental analyses and NMR and electrospray mass spectra (see the Supporting Information). The NMR shifts point to the diamagnetic nature of the complexes. Structural confirmation for the Cu^{III} corrolato complex **3** was obtained by single-crystal X-ray crystallography (Figure 1; see also the Supporting Information, Table S1). All of the bond distances and angles are comparable to those of previously reported Cu^{III} corrolato molecules.[15]

The central copper atom fits well into the cavity of the corrolato ring in a slightly distorted square planar geometry with a minimal deviation of 0.0301 Å from the N_4 plane. The distortion is due to slight deviations in the N-Cu-N bite angles in the range of 82.2–96.6° from the ideal ones. As a consequence, the pyrrole-ring nitrogen atoms are tilted with respect to the mean corrolato plane (19 atom corrole ring) by distances alternately varying from −0.133 Å to +0.252 Å. This saddled structure stabilizes the compound. The pyrrole rings alternately move down and up to accommodate the central metal atom, copper, and hence stabilize the structure (see the Supporting Information). The Cu–N distances in **3** lie between 1.873 Å and 1.907 Å and are at par with the earlier reported characteristic Cu^{III}–N bonds.[15] The substituted phenyl rings at the 5- and 15-meso-positions and the naphthyl group at the 10-position have been found to form dihedral angles of 42.5°, 58.5°, and 62.5° with the mean corrolato plane.

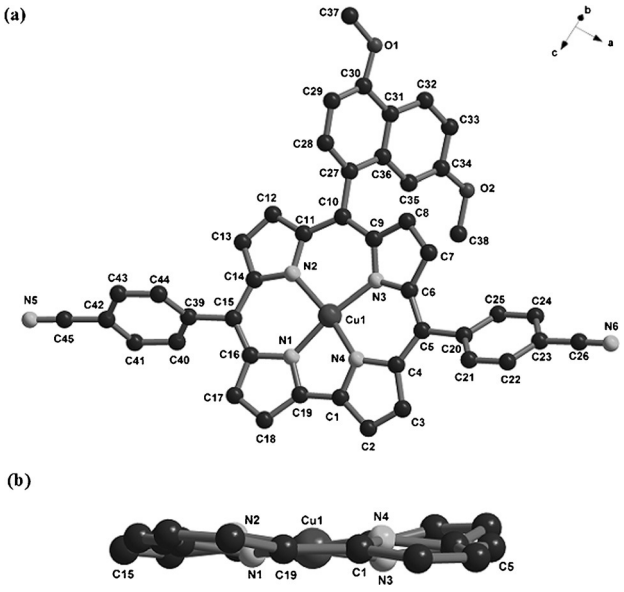

Figure 1. a) Single-crystal X-ray structure of **3**. Hydrogen atoms are omitted for clarity. b) Side view of the crystal structure of **3**, representing the saddling. All of the hydrogen atoms and the meso substituents have been removed for clarity).

XANES measurements[16] at the copper K-edge of complex **2** confirm the oxidation state of Cu^{III}. Two characteristic features (Figure 2) lead to this conclusion. A very weak pre-edge peak is detected at 8980.5 eV, while a more intense feature is observed in the edge at 8986.5 eV. Whereas the position of the first 1s→3d transition is an unambiguous diagnostic of Cu^{III}, the more intense 1s→4p + LMCT shake-down transition is more ligand-dependent and can only support the conclusion drawn from the weak quadrupole transition.[17]

The cyclic voltammograms and the differential pulse voltammograms of complexes **1**, **2**, and **3** were measured in CH_2Cl_2/0.1 M TBAP (see Figure S1 and Table S2). Each of the three copper complexes displayed one reversible oxidation and one reversible reduction step. The oxidation couple was

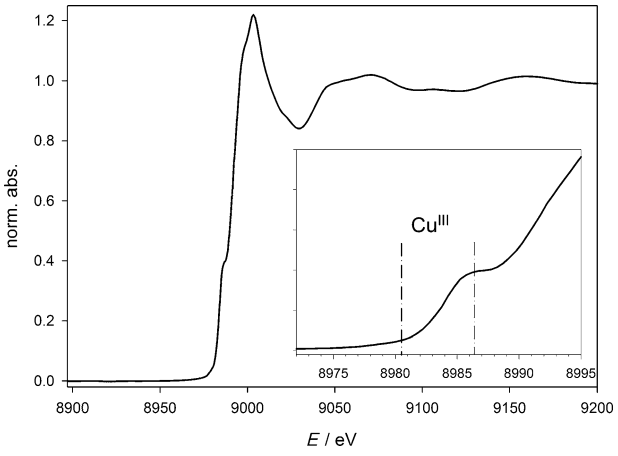

Figure 2. Cu K-edge XANES spectrum of complex **2**. The pre-edge area is shown in enlarged form in the inset.

observed at E^0_{298}, V (ΔE_p, mV): 0.41(80), 0.35(80), and 0.36(80) for **1**, **2**, and **3**, respectively, versus ferrocene/ferrocenium. These complexes also exhibited one reversible reductive couple E^0_{298}, V (ΔE_p, mV): −0.61(80) (**1**), −0.63(80) (**2**), and −0.64(90) (**3**) versus ferrocene/ferrocenium. In the series **1**→**2**→**3**, the electronic effects of various substituents on the aryl rings on their redox potential visibly appeared to be insignificant. The oxidation potentials of the copper complexes are similar to those of their silver analogues,[13] whereas the reduction potentials are shifted in the positive direction. To gain a more detailed knowledge of the electronic structures of these complexes and to ascertain the electronic structures in their various redox states, UV/Vis/NIR and EPR spectroelectrochemical measurements, combined with DFT and TD-DFT calculations, were performed.

As expected, no EPR signals were obtained for the diamagnetic native states of the three complexes (**1**–**3**). As the EPR spectrum of the one-electron-oxidized species of all three complexes have similar patterns and the same holds true for the one-electron-reduced species as well, we chose to discuss only of each in detail (see Figure 3 and Figure S2). The

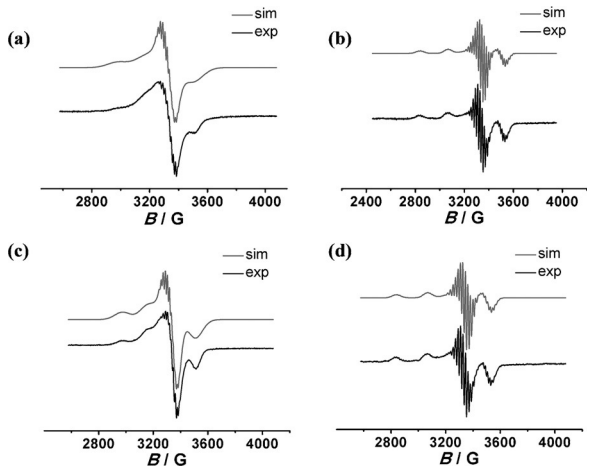

Figure 3. X-band EPR spectra of a) $\mathbf{2}^{\bullet+}$, b) $\mathbf{2}^{\bullet-}$, c) $\mathbf{3}^{\bullet+}$, and d) $\mathbf{3}^{\bullet-}$ with simulations by in situ electrolysis at 110 K in CH_2Cl_2/0.1 M Bu_4NPF_6.

EPR data of all of the complexes are presented in Table S3 a. The in situ generated one-electron-reduced species $\mathbf{3}^{\bullet-}$ in CH_2Cl_2/0.1 M Bu_4NPF_6 displays a typical Cu^{II}-type EPR spectrum (Figure 3 d). The spectra were also simulated with the Easyspin[18] software by considering an axial g tensor with $g_{//} = 2.127$ and $g_{\perp} = 2.034$. Furthermore, hyperfine and superhyperfine interactions were observed for the copper ($^{63,65}Cu$, $I = 3/2$) and nitrogen (^{14}N, $I = 1$) nuclei respectively. Simulation of the spectrum delivered an axial hyperfine tensor for Cu and a rhombic superhyperfine tensor for N. The values obtained for Cu are $A_{//} = 665$ and $A_{\perp} = 80$ MHz. The absolute values as well as their trends are in good agreement with known Cu^{II} EPR parameters. As expected, the coupling constants to the ^{14}N atoms are much smaller compared to those to Cu^{II} (see Table S3 a).

Structure-based calculations of the EPR spectra at the B3LYP/aug-cc-pVTZ-J level of theory reproduced the experimental results with reasonable accuracy with the calculated g tensors for $\mathbf{3}^{\bullet-}$ being $g_{//} = 2.104$ and $g_{\perp} = 2.034$. DFT delivered a slightly rhombic A tensor (albeit with two A values very close to each other, see Table S3). The trends in the A values are reproduced well by the calculations, with the calculated coupling constants being slightly lower than the experimental ones for copper. The spin densities calculated from the Löwdin population analysis indicated that about 64 % of the spin density resides on the copper center for the one-electron-reduced forms of the complexes (see Figure 4

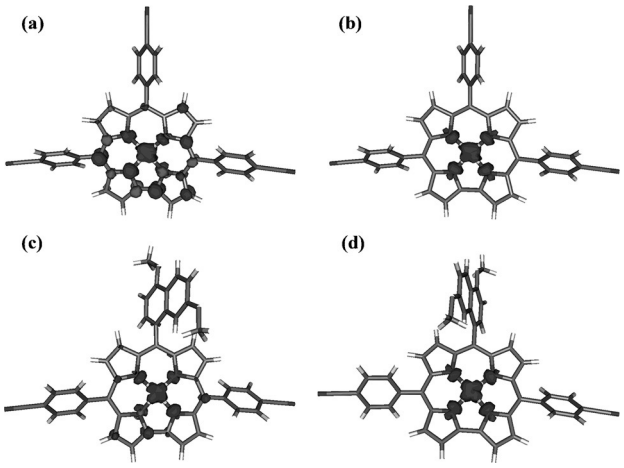

Figure 4. Spin-density representations for a) $\mathbf{1}^{\bullet+}$, b) $\mathbf{1}^{\bullet-}$, c) $\mathbf{3}^{\bullet+}$, and d) $\mathbf{3}^{\bullet-}$ (iso value 0.005).

and Table S3 b). Such a spin-density distribution is very similar to what has recently been reported by us for the Ag analogues of these copper complexes. The experimental EPR data, together with the DFT calculations, thus point to a major contribution of the $[(corrolato^{3-})Cu^{II}]^{\bullet-}$ form to the one-electron-reduced forms of these complexes, resulting in the usual formal Cu^{II} oxidation state.

The resolution of the spectrum for $\mathbf{1}^{\bullet+}$ is rather poor, and hence the data presented for that complex should be seen as approximate limits. However, for $\mathbf{2}^{\bullet+}$ and $\mathbf{3}^{\bullet+}$, the resolution of the spectra is good enough to allow the extraction of g and A tensors with reasonable accuracy. The in situ generated one-electron-oxidized species $\mathbf{3}^{\bullet+}$ in CH_2Cl_2/0.1 M Bu_4NPF_6 displays a pattern that also points to a predominantly copper-centered spin.[15] Simulation of the spectrum of $\mathbf{3}^{\bullet+}$ delivered an axial g tensor with values of $g_{//} = 2.089$ and $g_{\perp} = 2.035$. Additionally, the simulations delivered $A_{//} = 520$ and $A_{\perp} = 50$ MHz. Furthermore, superhyperfine couplings to the ^{14}N atoms were also considered for the simulations (see Table S3 a). The absolute values of the hyperfine coupling constants for copper and the superhyperfine coupling constants for ^{14}N are slightly larger for the reduced forms than for the oxidized forms. Nevertheless, the values obtained for $\mathbf{3}^{\bullet+}$ clearly point to a predominantly metal-centered spin. DFT calculations delivered a slightly rhombic g tensor for $\mathbf{3}^{\bullet+}$ with g values of 2.066, 2.026, and 2.023. However, the absolute values match reasonably well with the experimental values. The trends in the calculated A tensors for copper and nitrogen

match reasonably well with the experimental results, and the calculations also deliver smaller values for the hyperfine coupling constant to copper than for the reduced species (see Table S3 a). A look at the spin densities calculated using the Löwdin population analysis for $\mathbf{3}^{\bullet+}$ shows that 44 % of the spin density is located on the corresponding copper atom (see Figure 4 and Table S3 b). For the corresponding silver complexes, less than 1 % of the spin density was located at the metal center for the oxidized forms,[13] leading to their description as $[(\text{corrolato}^{\bullet 2-})\text{Ag}^{\text{III}}]^{\bullet+}$. For the present case, both the experimental EPR spectra as well as spin density data thus clearly establish that formulations with significant spin density on the copper center are required to correctly describe the oxidized species.

As the electronic spectra of **2** and **3** in all redox states are virtually identical, only those of **1** and **3** will be discussed in detail (see Figure 5 and Figure S3). The native states of the

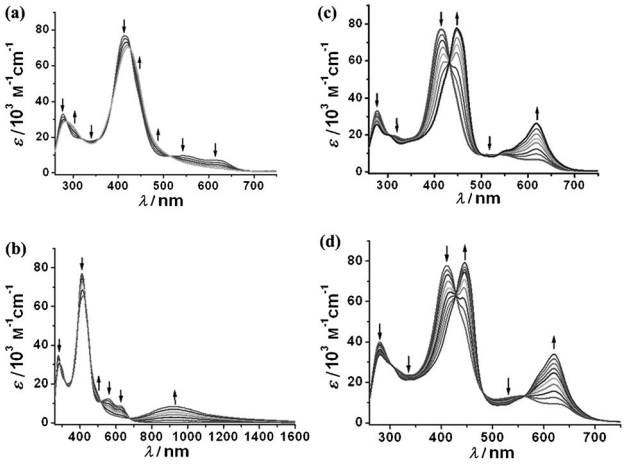

Figure 5. Changes in the UV/Vis/NIR spectrum of a) **1** and b) **3** during the first oxidation, and c) **1** and d) **3** during the first reduction. Results from OTTLE spectroelectrochemistry in CH_2Cl_2/0.1 M Bu_4NPF_6.

complexes display typical spectra expected for a neutral Cu corrolato species.[19] The Soret bands were observed for all cases, and the positions of these bands are hardly influenced by the substituents on the corrolato rings (see the Supporting Information). Details of the interpretation obtained through TD-DFT calculations are given in Tables S4–S9 and Figures S4–S9.

Upon one-electron reduction of **1** to $\mathbf{1}^{\bullet-}$, all of the bands in the visible region are shifted to lower energies (see Table S10). Similarly, upon the one-electron reduction of **3** to $\mathbf{3}^{\bullet-}$, the Soret band decreases in intensity and finally disappears giving rise to a new band of higher intensity at a longer wavelength of 446 nm. The other low-energy bands in the visible region also decrease in intensity along with the development of a new intense band at 620 nm. Such a spectral change matches well with the metal-centered reduction processes reported earlier in related corrolato Cu^{III} complexes (Figure 5).[20] Contributions from HOMO-2α→LUMOα, HOMOα→LUMOα, and HOMOβ→LUMOβ were found for this transition (see the Supporting Information). The origin of the band at 620 nm was thus calculated by TD-DFT to be a mixture of ILCT and MLCT transitions. Similar bands are also observed for $\mathbf{1}^{\bullet-}$.

Upon one-electron reduction, the formal Cu^{II} centers are relatively electron-rich, and MLCT transitions thus become highly feasible. The most prominent change in the UV/Vis/NIR spectra of these complexes upon one-electron oxidation is the appearance of long-wavelength bands, particularly for $\mathbf{2}^{\bullet+}$ and $\mathbf{3}^{\bullet+}$, in the NIR region (see Figure S3 and Figure 5). These bands appear at 947 nm and 921 nm for $\mathbf{2}^{\bullet+}$ and $\mathbf{3}^{\bullet+}$, respectively. Upon the one-electron oxidation of Cu^{III} corroles, such bands in the NIR region have never been reported before.

The origin of this new low-energy band can be explained with the help of TD-DFT calculations and has contributions, among others, from HOMO-2α→LUMOα and HOMO-1β→LUMOβ transitions (see the Supporting Information). This low energy band is a manifestation of mixed ILCT and LMCT transitions (see Figure S7 and Table S7). For $\mathbf{1}^{\bullet+}$, no such bands in the NIR region were experimentally detected, and TD-DFT calculations also do not predict any NIR bands for this structure. Such an observation would fit with the proposed LMCT character of the band, with the substituents on the backbone of the corrolato ligands in $\mathbf{2}^{\bullet+}$ and $\mathbf{3}^{\bullet+}$ being responsible for a smaller energy gap between the relevant orbitals, an effect that is missing for $\mathbf{1}^{\bullet+}$. The changes in the Soret bands upon one-electron oxidation of these species are minimal (Figure 5).

DFT geometry optimizations were performed to get insights into this phenomenon. Three different cases, namely a singlet, a triplet, and a broken-symmetry case, were calculated using the BP 86 functional. The calculated saddling values for the singlet and the broken symmetry cases match reasonably well with the experimental values (see Table S11). Calculations for the triplet state delivered an almost flat structure, confirming that the ground state of the corrolato Cu^{III} complexes is indeed the singlet state (as has been experimentally observed). To exclude functional-dependent errors as a source of the saddling, we also used higher-generation (OLYP) and hybrid (B3LYP) functionals to look into the saddling effect for the singlet case, but all functionals, with or without empirical van der Waals corrections, delivered a saddled structure (see Table S11). This saddling, which has been invoked to account for electron flow from the corrolato unit to the $d_{x^2-y^2}$ orbital of the copper center, has important consequences for the formal oxidation state in these complexes (non-innocent character of the corrolato unit).[19,21–23] The $d_{x^2-y^2}$ orbitals of copper are closer in energy to the corrolato-based orbitals than those of their silver and gold homologues. This fact leads to a situation where extensive overlap between the copper $d_{x^2-y^2}$ and the corrolato orbitals occurs (higher covalency!), which is not observed for its higher homologues. As a result, no saddling of the corrolato structure is usually observed in complexes of the higher homologues of the coinage metal copper. The saddling introduces a certain Cu^{II} character into the otherwise formal corrolato Cu^{III} complexes.[19,21–23] Interestingly, a certain amount of saddling was also calculated for the oxidized and reduced forms of the complexes, and the saddling effect for

those redox forms also turned out to be independent of the functional used (see the Supporting Information). For the native state of the complexes, the formal cor^{3-} ligand has two electrons (for a dative bond) and the formal Cu^{III} center has two holes (empty $d_{x^2-y^2}$ orbital), rendering electron flow from cor^{3-} to Cu^{III} possible and saddling unavoidable. As saddling is also observed for the oxidized and reduced forms, electrons on the corrolato ligand and holes on the copper center should be present to make the saddling happen. Thus, we feel that forms such as $(cor)^{-}$ and Cu^{I} are less likely to contribute to the various redox forms of these copper complexes.

As discussed above, the reduced forms of the copper complexes described here as well as the silver analogues previously reported by us display a predominantly metal-centered spin, with a Cu^{II} or Ag^{II} formulation being appropriate. For the oxidized forms, however, both experiment and theory deliver large spin densities on the copper center whereas for the silver analogues, no spin density was detected at the metal center. This difference has interesting consequences for the formal oxidation state distributions in these complexes (Scheme 1).

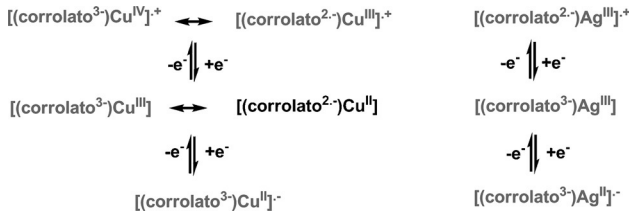

Scheme 1. Formal oxidation states for the various redox states in corrolato copper complexes (left) and their silver analogues (right), which we recently reported.[13] Species that contribute significantly are shown in gray.

Therefore, for the oxidized species, formulations with spin on the copper center are necessary (Scheme 1) to correctly depict the electronic structure, which were not required for the oxidized silver complexes. Such a situation thus renders contributions from Cu^{IV} relevant in the present case. An alternative formulation with Cu^{II} will contain a doubly oxidized mononegative corrolato ligand. We feel that such a form will not make significant contributions to the electronic structure.

It needs to be mentioned that redox-induced electron transfer has been invoked earlier for metal complexes of non-innocent ligands. Surprisingly, the copper complexes display a more mixed orbital situation compared to the silver ones. For most metal complexes, higher covalency is usually observed for the higher homologues. This fact is likely related to the structural saddling discussed above. The copper complexes thus provide an ideal platform for investigating reactivity with metal–ligand cooperativity.[24]

In conclusion, we have discussed the various redox states of corrolato copper complexes in comparison to their silver analogues. This is the first spectroscopic and structural characterization of the oxidized forms of corrolato copper complexes. We have used a combination of structural, electrochemical, spectroelectrochemical, and theoretical methods to show that the native states of these complexes can best be described as a mixture of Cu^{II} and Cu^{III}, a fact that was recognized earlier in the literature and is different from their silver analogues. The reduced forms of both species can best be described as divalent metal centers. Finally, the oxidized forms show interesting differences. Whereas the oxidized silver complex can be exclusively formulated as a Ag^{III} species bound to a dianionic corrolato radical, the copper analogues present a more complicated and intriguing feature. Cu^{IV} should indeed be invoked to correctly describe the electronic structure of that redox state. Surprising, a more mixed-orbital situation is observed for the copper complexes than for their silver analogues. This fact is contrary to what is usually observed for metal complexes of non-innocent ligands.[25–30] The more mixed situation observed for the copper complexes should thus lead to interesting reactivity patterns, where metal–ligand cooperativity[24] can be used for bond activation and catalysis.

Acknowledgements

Financial support received from the Department of Atomic Energy (India) is gratefully acknowledged. We acknowledge NISER-Bhubaneswar for providing infrastructure. The Fonds der chemischen Industrie (FCI) is kindly acknowledged for financial support. We are grateful to the Fonds der Chemischen Industrie (Chemiefondsstipendium to M.G.S.) and the Carl-Zeiss Stiftung (doctoral stipend to N.D.) for financial support of this work. The high-performance computing facilities at ZEDAT, FU Berlin are acknowledged for access to computing resources. M.B. thanks the DFG for support within the Forschergruppe 1405.

Keywords: copper corroles · EPR spectroscopy · higher oxidation states · spectroelectrochemistry · XANES measurements

How to cite: *Angew. Chem. Int. Ed.* **2015**, *54*, 13769–13774
Angew. Chem. **2015**, *127*, 13973–13978

[1] a) C. K. Jørgensen, C. K. Jørgensen, *Oxidation numbers and oxidation states*, Springer, Berlin-Heidelberg-New York, **1969**; b) R. Sheldon, *Metal-Catalyzed Oxidations of Organic Compounds*: *Mechanistic Principles and Synthetic Methodology Including Biochemical Processes*, Elsevier, **2012**.
[2] G. Wang, M. Zhou, J. T. Goettel, G. J. Schrobilgen, J. Su, J. Li, T. Schlöder, S. Riedel, *Nature* **2014**, *514*, 475–477.
[3] S. M. Barnett, K. I. Goldberg, J. M. Mayer, *Nat. Chem.* **2012**, *4*, 498–502.
[4] X. Ribas, A. Casitas, B. Pignataro, *Ideas in Chemistry and Molecular Sciences: Where Chemistry Meets Life*, Wiley-VCH, Weinheim, **2010**.
[5] H. Maeda, A. Osuka, H. Furuta, *J. Am. Chem. Soc.* **2003**, *125*, 15690–15691.
[6] G. Chen, J.-M. Langlois, Y. Guo, W. A. Goddard, *Proc. Natl. Acad. Sci. USA* **1989**, *86*, 3447–3451.
[7] A. J. Hickman, M. S. Sanford, *Nature* **2012**, *484*, 177–185.
[8] N. W. Aboelella, S. V. Kryatov, B. F. Gherman, W. W. Brennessel, V. G. Young, R. Sarangi, E. V. Rybak-Akimova, K. O. Hodgson, B. Hedman, E. I. Solomon, *J. Am. Chem. Soc.* **2004**, *126*, 16896–16911.

[9] W. Harnischmacher, R. Hoppe, *Angew. Chem. Int. Ed. Engl.* **1973**, *12*, 582 – 583; *Angew. Chem.* **1973**, *85*, 590 – 590.
[10] M.-T. Zhang, Z. Chen, P. Kang, T. J. Meyer, *J. Am. Chem. Soc.* **2013**, *135*, 2048 – 2051.
[11] E. Vogel, S. Will, A. S. Tilling, L. Neumann, J. Lex, E. Bill, A. X. Trautwein, K. Wieghardt, *Angew. Chem. Int. Ed. Engl.* **1994**, *33*, 731 – 735; *Angew. Chem.* **1994**, *106*, 771 – 775.
[12] Z. Gross, *J. Biol. Inorg. Chem.* **2001**, *6*, 733 – 738.
[13] W. Sinha, M. G. Sommer, N. Deibel, F. Ehret, B. Sarkar, S. Kar, *Chem. Eur. J.* **2014**, *20*, 15920 – 15932.
[14] K. M. Kadish, V. A. Adamian, E. Van Caemelbecke, E. Gueletii, S. Will, C. Erben, E. Vogel, *J. Am. Chem. Soc.* **1998**, *120*, 11986 – 11993.
[15] C. Brückner, R. P. Briñas, J. A. K. Bauer, *Inorg. Chem.* **2003**, *42*, 4495 – 4497.
[16] A. B. Ene, M. Bauer, T. Archipov, E. Roduner, *Phys. Chem. Chem. Phys.* **2010**, *12*, 6520 – 6531.
[17] J. L. DuBois, P. Mukherjee, A. M. Collier, J. M. Mayer, E. I. Solomon, B. Hedman, T. D. P. Stack, K. O. Hodgson, *J. Am. Chem. Soc.* **1997**, *119*, 8578 – 8579.
[18] S. Stoll, A. Schweiger, *J. Magn. Reson.* **2006**, *178*, 42 – 55.
[19] I. H. Wasbotten, T. Wondimagegn, A. Ghosh, *J. Am. Chem. Soc.* **2002**, *124*, 8104 – 8116.
[20] Z. Ou, J. Shao, H. Zhao, K. Ohkubo, I. H. Wasbotten, S. Fukuzumi, A. Ghosh, K. M. Kadish, *J. Porphyrins Phthalocyanines* **2004**, *8*, 1236 – 1247.
[21] A. B. Alemayehu, E. Gonzalez, L. K. Hansen, A. Ghosh, *Inorg. Chem.* **2009**, *48*, 7794 – 7799.
[22] K. E. Thomas, A. B. Alemayehu, J. Conradie, C. M. Beavers, A. Ghosh, *Acc. Chem. Res.* **2012**, *45*, 1203 – 1214.
[23] M. Bröring, F. Bregier, E. Cónsul Tejero, C. Hell, M. C. Holthausen, *Angew. Chem. Int. Ed.* **2007**, *46*, 445 – 448; *Angew. Chem.* **2007**, *119*, 449 – 452.
[24] a) V. Lyaskovskyy, B. de Bruin, *ACS Catal.* **2012**, *2*, 270 – 279; b) S. Kundu, E. Miceli, E. Farquhar, F. F. Pfaff, U. Kuhlmann, P. Hildebrandt, B. Braun, C. Greco, K. Ray, *J. Am. Chem. Soc.* **2012**, *134*, 14710 – 14713; c) S. Alesi, G. Brancolini, M. Melucci, M. L. Capobianco, A. Venturini, N. Camaioni, G. Barbarella, *Chem. Eur. J.* **2008**, *14*, 513 – 521; d) O. Reinaud, P. Capdevielle, M. Maumy, *Chem. Commun.* **1990**, 566 – 568; e) P. Comba, S. Knoppe, B. Martin, G. Rajaraman, C. Rolli, B. Shapiro, T. Stork, *Chem. Eur. J.* **2008**, *14*, 344 – 357.
[25] P. J. Chirik, *Inorg. Chem.* **2011**, *50*, 9737 – 9740.
[26] W. Kaim, *Inorg. Chem.* **2011**, *50*, 9752 – 9765.
[27] R. Eisenberg, H. B. Gray, *Inorg. Chem.* **2011**, *50*, 9741 – 9751.
[28] K. G. Caulton, *Eur. J. Inorg. Chem.* **2012**, 435 – 443.
[29] H. Grützmacher, *Angew. Chem. Int. Ed.* **2008**, *47*, 1814 – 1818; *Angew. Chem.* **2008**, *120*, 1838 – 1842.
[30] C. Gunanathan, D. Milstein, *Acc. Chem. Res.* **2011**, *44*, 588 – 602.

Received: August 6, 2015
Published online: September 25, 2015

